*Journal of Engineering Mathematics* **39:** 345–366, 2001


# Asymptotic analysis of the flow of shear-thinning foodstuffs in annular scraped heat exchangers

A D FITT and C. P. PLEASE
*Faculty of Mathematical Studies, University of Southampton, Southampton SO17 1BJ, UK (e-mail: adf@maths.soton.ac.uk; cpp@maths.soton.ac.uk)*

Received 22 February 2000; accepted in revised form 10 August 2000

**Abstract.** The problem of isothermal flow of a shear-thinning (pseudoplastic) fluid in the gap between two concentric cylinders is considered. A pump provides an axial pressure gradient which causes flow down the device. The outer cylinder is fixed and has 'scrapers' attached to it to cause flow mixing, whilst the inner cylinder rotates about its axis to provide shear and thus thin the fluid. The goal is to determine the optimal distribution of power between rotation and pumping. Although ostensibly the flow is nonlinear and three-dimensional we show that judicious use of fairly straightforward asymptotic methods can yield a great deal of information about the device, including cross-sectional flow predictions and throughput results. Furthermore, these results are derived for a variety of different flow conditions. Some numerical calculations are carried out using a commercial CFD code. These show good agreement with the asymptotic analysis.

**Key words:** asymptotic analysis, food industry, lubrication theory, shear-thinning fluids, slow flow

## 1. Introduction

In this study we discuss a problem connected with a process commonly employed in the food manufacturing industry. Since the problem ostensibly concerns a non-Newtonian fluid flowing in a complex, moving geometrical region in three dimensions, one might expect that the only way of deriving results of any practical use would be to proceed along purely numerical lines. We shall show, however, that by judicious use of asymptotic analysis the problem *as originally posed* may be virtually completely solved. It is the nature of real-world problems that when questions about an industrial process are posed and answered, inevitably they lead only to additional more detailed and difficult questions; we shall indicate how further aspects of the problem may be examined and what mathematical and numerical tools might be utilised.

It is worth emphasising that one's expectations of what asymptotic analysis might be able to achieve for practical problems must be constantly tempered with experience and realism. It would be absurd to suggest that all problems may be completely solved using asymptotic analysis alone. In most industrial settings it will eventually be necessary to employ numerical computation to fully analyse a process. This computation may be carried out using purpose-designed software or 'black box' CFD packages. This study should therefore be thought of as in no way belittling the role that numerical analysis has to play; rather it puts forward the views that (i) a great deal of insight can be gained from carrying out carefully considered asymptotic analysis and (ii) that in an ideal world *a combination* of asymptotic and numerical analysis should be used to attack a given problem.

In order to illustrate how effective asymptotic analysis can be in tackling complicated problems it is tempting to "invent" a superficially practical problem where all of the para-

meter values are chosen so that asymptotic analysis succeeds in every subproblem. We have resisted this temptation however and considered a real industrial problem as presented by a real industrial company. Although the fluid mechanics, rheology and asymptotic analysis that are required to make progress are not in themselves too testing, the problem provides a graphic illustration of the power of asymptotics.

### 1.1. Industrial background

The problem discussed below was brought to our attention during a meeting between representatives from Crown Chemtech Ltd. (a small company based in Reading, Berkshire, UK which makes machinery for food processing), members of the Food Sciences Group at the University of Reading and members of the Departments of Mathematics at the Universities of Reading and Southampton.

In its simplest form, the problem may be stated thus: a fatty oil flows in the annular gap between two concentric circular cylinders, driven by a known axial pressure gradient: predict the throughput for given device parameters. In the current setting, however, a number of complicating factors arise. Firstly, the fatty fluid is to be turned (for example) into margarine. Essentially, this is done by cooling the fluid as it progresses down the annulus, which therefore acts as a heat exchanger. At the upstream end of the device, the product may thus truly be regarded as a fluid, but at exit it more resembles a paste. Secondly, the fluid is non-Newtonian and has a temperature-dependent viscosity. In particular, it is known that a good model for the rheology of the fluid is to assume that it is a power-law shear-thinning fluid with zero yield stress and a known shear-thinning exponent. Thirdly, the inner cylinder rotates with a given angular velocity $\Omega$ and the outer cylinder has a number of 'scrapers' (knife blades) that are attached normally to it.

Clearly there are many different aspects of this problem that could be studied. In the first instance, however, our industrial partner wished to neglect altogether the impact of the heat exchange process on the flow, and consider the whole process to be isothermal. (Details of the thermal problem may be found in [1] ) Also, it was clear that, although the present device was concerned with the manufacture of margarine, it could also be used for a wide range of other food products, including molten chocolate, jam, jelly and spreads such as peanut butter (all of which may be considered to be power-law shear-thinning fluids with a zero yield stress ([2]))

The shear-thinning nature of liquid food products has an important effect on the prediction and optimisation of device throughput, since it may be exploited to increase production. Indeed, if the flow in such devices were to be generated *only* by a pressure gradient, it is known that unacceptably large pressure gradients would be required to achieve the desired throughput. The general idea therefore is to divert some energy away from the pumps producing the pressure gradient in the annulus and use it instead to rotate the inner cylinder. Evidently by doing this the shear in the fluid will be increased, leading to a thinning of the fluid that will greatly ease its passage down the device.

In the absence of heat transfer, we shall therefore suppose that a given amount of power is available to run the device and assume that the point at issue is one of optimisation, namely how much of the power should be used for rotation of the inner cylinder and how much should be invested in producing a pressure gradient from the pump. (Evidently an optimum use of energy must exist, for whilst *some* rotation of the inner cylinder is known to increase the throughput it is clear that if all of the energy were to be used in cylinder rotation then the throughput would be zero.)

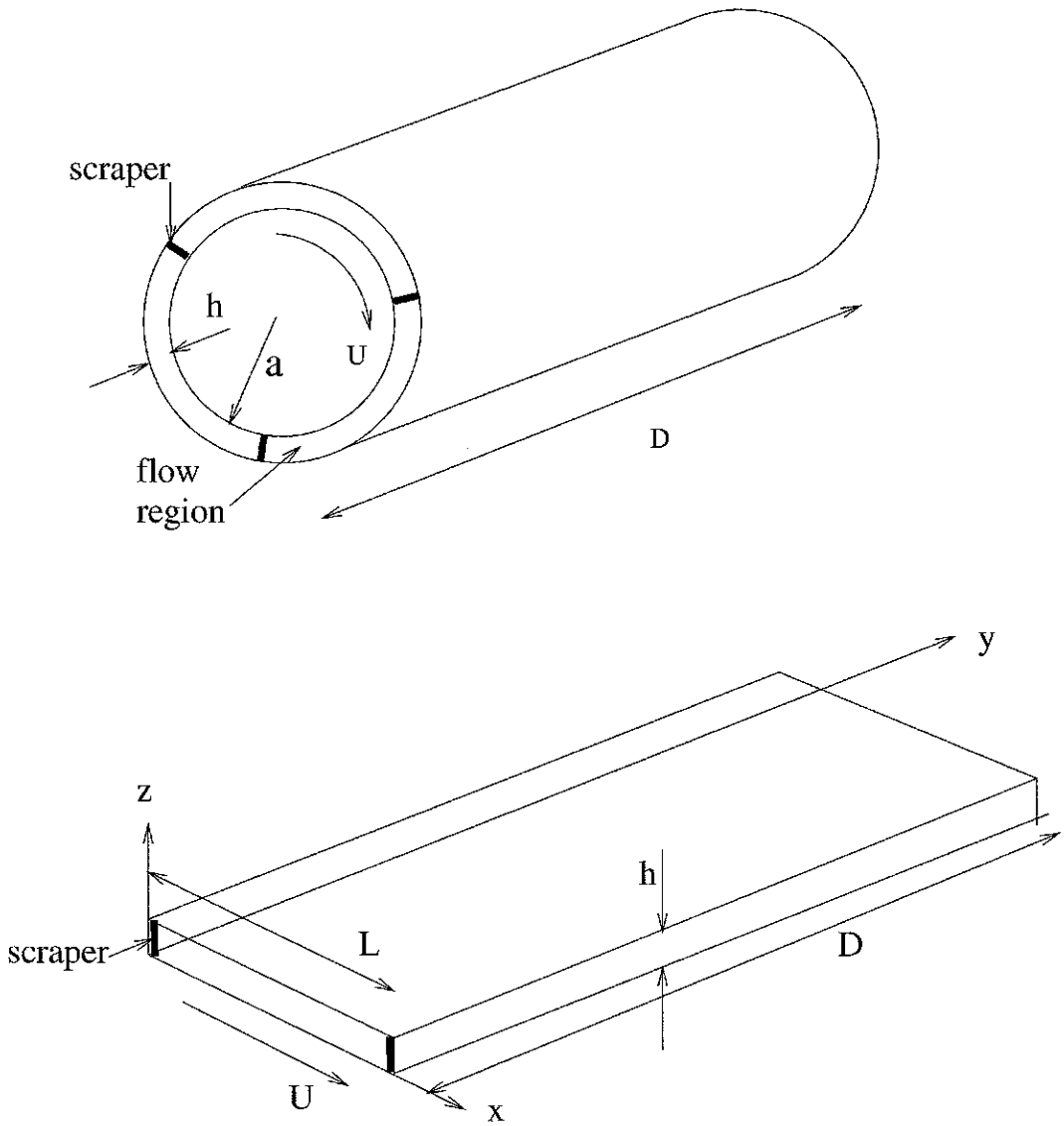


*Figure 1* (Top) Schematic view of device (bottom) schematic view of 'unwrapped' device.

## 2. Mathematical modelling

Schematic diagrams of the device and the coordinate system that will be employed are shown in Figure 1. The radius of the inner cylinder is denoted by $a$, the (linear) rotation speed of the inner cylinder by $U = \Omega a$, the length of the device by $D$, and the annular gap width by $h$. We also denote the 'unwrapped' distance between two scrapers by $L$. Kinematic viscosity and density are denoted by $\nu$ and $\rho$, respectively, and $t_R$ and $V$ denote a typical residence time in the machine and a typical speed in the $y$-direction, respectively.

## 2.1. NUMERICAL PROBLEM

We begin by stating the full problem. This would have to be solved numerically if we decided to analyse the device without using any form of theoretical or asymptotic analysis.

The flow is governed by the three-dimensional unsteady Navier-Stokes equations

$$\rho \frac{\mathrm{d}\boldsymbol{q}}{\mathrm{d}t} = \operatorname{div} T, \tag{1}$$

$$\operatorname{div} \boldsymbol{q} = 0, \tag{2}$$

where the fluid velocity is denoted by $\boldsymbol{q}$, $T$ is the stress tensor and we have assumed that there are no body forces. Following the information given, we treat the fluid as an isothermal shear-thinning fluid with zero yield stress and use the constitutive law (see, for example [3, p. 55])

$$T = -p\delta_{ij} + \Lambda \mid (d_{kl}d_{kl})^{\frac{m-1}{2}} \mid 2d_{ij}, \tag{3}$$

where $p$ denotes pressure, $d_{ij}$ is the infinitesimal rate-of-strain tensor given by

$$d_{ij} = \tfrac{1}{2}(\nabla \boldsymbol{q} + \nabla \boldsymbol{q}^T),$$

$m \in (0, 1]$ is the 'shear-thinning index' (the model is still valid for shear *thickening* fluids such as corn starch where $m > 1$, but we do not pursue this further here) and $\Lambda$ is a constant that is usually referred to as the 'consistency' of the fluid (which has dimensions $\mathrm{s}^{m-2}\ \mathrm{kg\ m}^{-1}$).

The full numerical problem thus consists of solving the Equations (1) and (2) with the constitutive law (3), subject to the boundary conditions

$$\boldsymbol{q} = 0 \quad \text{at} \quad r = a + h; \quad \boldsymbol{q} = U\boldsymbol{e}_\theta \quad \text{at} \quad r = a,$$

(where $\boldsymbol{e}_\theta$ is a unit vector in the $\theta$-direction),

$$\boldsymbol{q} = 0 \quad \text{on the surface of each scraper.}$$

To complete the problem specification, it is also necessary to prescribe suitable initial conditions and to specify conditions at $y = 0$ and $y = D$.

Evidently the numerical problem is demanding. Even if we avoid consideration of start-up and spin-down processes and examine only steady flow, the problem is essentially three-dimensional and contains moving boundaries. The boundary conditions that must be imposed at the ends $y = 0$ and $y = D$ of the device are awkward, for though it might not be too hard to enforce a zero stress condition at $y = D$, the correct condition at the inlet to the device seems to be that the normal stress is given (in practice this is probably what would be measured as the 'pressure') and the other two components of the stress are zero. At the inlet, therefore, no velocity profiles are known. The numerical problem also involves all the usual complications due to the convective derivative terms and the fact that the pressure occurs in the equations only in the guise of a Lagrange multiplier. Furthermore, the nonlinearity of the fluid must be taken into consideration. There are a number of 'black box' commercial codes that claim to be able to successfully carry out calculations of this sort, but even with the power of today's PCs, it is doubtful whether three-dimensional runs would be able to be carried out in the sort of execution times that would make parametric studies possible.

As an alternative to large-scale computing, we therefore examine the problem from an asymptotic-analysis point of view. It is worth observing that, though some previous authors have concerned themselves with two-dimensional lubrication theory for slider bearings (see, for example [4–7]), not much attention seems to have been given to three-dimensional problems involving shear-thinning fluid flow. The flow of a Bingham fluid in eccentric annular geometries was studied in [8] in a case where the inner cylinder was at rest. The resulting simple shear profile allowed mathematical progress to be made. A modification of this study was presented in [9], where a system with concentric cylinders was examined but the inner cylinder was allowed to rotate. Analytical progress could be made for a paradigm problem with a one-dimensional shear dependence, but for the general problem a numerical solution was required. Both [8] and [9] addressed the problem of the existence or otherwise of plug flow regions.

## 3. Asymptotic analysis

We begin by examining the sizes of the typical problem parameters and non-dimensionalizing (1) and (2). According to the device parameters supplied by Crown Chemtech. Ltd ,

$$U \sim 2\ \mathrm{m\,s^{-1}}, \quad h \sim 0{\cdot}015\ \mathrm{m}, \quad D \sim 2\ \mathrm{m}, \quad a \sim 0{\cdot}075\ \mathrm{m},$$

$$\nu \sim 0{\cdot}1\ \mathrm{m^2\,s^{-1}}, \quad \rho \sim 800\ \mathrm{kg\,m^{-3}},$$

so that the cylinder circumference is about 0·47 m. Assuming (since this is the standard configuration) that there are three scrapers, we thus have

$$L \sim 0{\cdot}15\ \mathrm{m}.$$

A typical residence time $t_R$ is about 10s and hence

$$V \sim 0\,2\ \mathrm{m\,s^{-1}}.$$

We scale according to $t = (L/U)\bar{t}$, $x = L\bar{x}$, $y = (L/\epsilon)\bar{y}$, $z = \epsilon L\bar{z}$, $u = U\bar{u}$, $v = \epsilon U\bar{v}$, $w = \epsilon U\bar{w}$ where $\epsilon = h/L$ and the bars denote non-dimensional quantities. The scalings for $t$, $u$, $w$, $x$ and $z$ are straightforward, and those used for $v$ and $y$ (which are motivated by the fact that the pipe is long compared to its radius) lead to a distinguished limit that is suggested by the values of the physical parameters in the problem. We also anticipate that lubrication theory-type analysis will be appropriate and set $p = (U/h)^{m-1}(\mu_0 U/L\epsilon^2)\bar{p}$ where for convenience we have defined $\mu_o = \Lambda 2^{(1-m)/2}$.

The next task is to insert the above scalings into (1) and (2) and determine the dominant terms in the equations. This procedure should be carried out on the full shear-thinning Navier–Stokes equations in cylindrical coordinates. We omit the details of this as they are well-known and simply note the result, which is that the (dimensional) leading-order problem is

$$0 = -p_x + (\mu_0(u_z^2)^{\frac{m-1}{2}}u_z)_z, \tag{4}$$

$$0 = -p_y + (\mu_0(u_z^2)^{\frac{m-1}{2}}v_z)_z, \tag{5}$$

$$0 = -p_z, \tag{6}$$

$$0 = u_x + w_z, \tag{7}$$

these equations being valid under the assumptions that

$$\epsilon \ll 1, \quad \epsilon^2 \mathrm{Re} \ll 1,$$

where the equivalent of the Reynolds number for shear-thinning flow is defined by

$$\mathrm{Re} = \frac{LU\rho}{\mu_0}\left(\frac{h}{U}\right)^{m-1}.$$

In the interests of clarity, all subsequent equations will be presented in dimensional form.

With the parameter values suggested above, (assuming Newtonian flow with $m = 1$ and $\mu_0/\rho = \nu$) we find that

$$\epsilon \sim 10^{-1}, \quad \mathrm{Re} \sim 3 \quad \epsilon^2 \mathrm{Re} \sim 0{\cdot}03,$$

thus justifying the neglect of the other terms in the full equations. Inertia is absent from (4–7) (which apply for either steady or unsteady flow, though we shall only consider steady flow), the leading-order balance being between viscous forces and the pressure gradient. All centrifugal forces are absent. One other point concerning (4–7) is worthy of note: although for convenience we have omitted the modulus signs in the viscosity terms, it is understood that the viscosity must be positive, so that some care must be taken whenever terms such as $\sqrt{u_z^2}$ are simplified.

We now proceed to solve (4–7) with appropriate boundary conditions. The fact that $p$ is independent of $z$ allows (4) to be solved with little difficulty; we divide the region $0 \leq z \leq h$ into two subregions $[0, z_c]$ and $[z_c, h]$ where $z_c$ (which is to be determined) is defined so that $u_z \leq 0$ for $z \in [0, z_c]$ and $u_z \geq 0$ for $z \in [z_c, h]$ (see Figure 2 for a typical velocity profile). Solving the $x$-momentum equation (4) by integration, we impose the boundary conditions

$$u_z(x, y, z_c) = 0, \quad u(x, y, 0) = U, \quad u(x, y, h) = 0.$$

This shows that

$$u = \begin{cases} \left(\dfrac{m}{1+m}\right)\left(\dfrac{p_x}{\mu_0}\right)^{\frac{1}{m}} [(z_c - z)^{\frac{1+m}{m}} - z_c^{\frac{1+m}{m}}] + U \quad (z \leq z_c) \\ \left(\dfrac{m}{1+m}\right)\left(\dfrac{p_x}{\mu_0}\right)^{\frac{1}{m}} [(z - z_c)^{\frac{1+m}{m}} - (h - z_c)^{\frac{1+m}{m}}] \quad (z \geq z_c) \end{cases} \tag{8}$$

We must also ensure that $u$ is continuous at $z = z_c$; this gives

$$\left(\frac{m}{1+m}\right)\left(\frac{p_x}{\mu_0}\right)^{\frac{1}{m}} (z_c^{\frac{1+m}{m}} - (h - z_c)^{\frac{1+m}{m}}) = U, \tag{9}$$

which we shall return to presently.

At this point, two elements are missing from the model, for $p_x$ is yet to be determined and the effect of the scrapers has not yet been considered. The pressure gradient is easily determined in the normal way by using the (continuity) equation (7). By integrating from $z = 0$ to $h$, we find that, since $w$ is zero on both $z = 0$ and $z = h$, we have

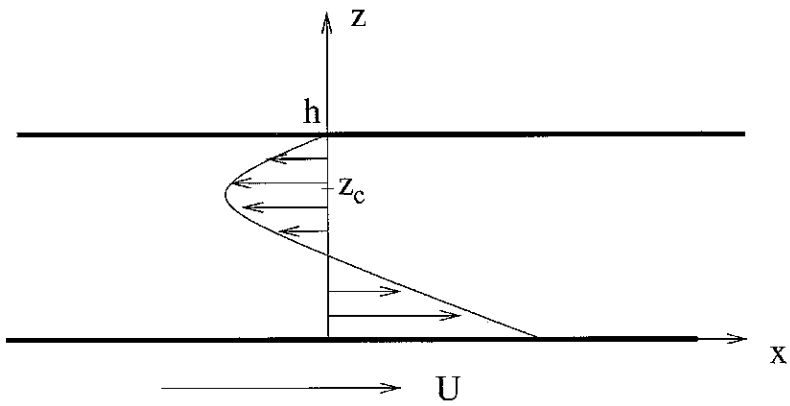


*Figure 2* Typical velocity profile for flow in annular gap between scrapers.

$$\int_0^h u_x \, dz = 0 \tag{10}$$

and thus (using (8))

$$\left(\frac{1}{1+m}\right)\left(\frac{1}{\mu_0}\right)^{\frac{1}{m}} p_x^{\frac{1}{m}-1} p_{xx} I_0 = 0,$$

where $I_0$ is an integral which is not zero. Thus $p_{xx} = 0$ and so $p_x$ is independent of $x$.

Now we consider the effect of the scrapers: we assume that each scraper does not allow flow across it (though see Section 5) and restricts the fluid between scrapers to that region To model the scrapers in a form suitable for lubrication theory we therefore impose the weaker condition that

$$\int_0^h u \, dz = 0 \tag{11}$$

at $x = 0$ and $x = L$ (Of course, lubrication theory is not valid in regions immediately adjacent to scrapers; here, where the flow changes direction, the full Navier Stokes equations with the appropriate boundary conditions must be solved. This will make no appreciable difference to the throughput qualities of the device, however. Lubrication theory may also not be valid near to the input and output regions of the device.) Applying (11) to (8) now gives

$$\left(\frac{m}{1+2m}\right)\left(\frac{p_x}{\mu_0}\right)^{\frac{1}{m}} [-z_c^{\frac{1+2m}{m}} - (h-z_c)^{\frac{1+2m}{m}}] + U z_c = 0 \tag{12}$$

and when (9) is combined with (12), we find that

$$1 = \frac{z_c(1+2m)[z_c^{\frac{1+m}{m}} - (h-z_c)^{\frac{1+m}{m}}]}{(1+m)[z_c^{\frac{1+2m}{m}} + (h-z_c)^{\frac{1+2m}{m}}]}.$$

The position $z_c$ is thus determined *only* by the shear-thinning index $m$ and satisfies

$$1 = \frac{\lambda(1+2m)[\lambda^{\frac{1+m}{m}} - (1-\lambda)^{\frac{1+m}{m}}]}{(1+m)[\lambda^{\frac{1+2m}{m}} + (1-\lambda)^{\frac{1+2m}{m}}]}, \tag{13}$$

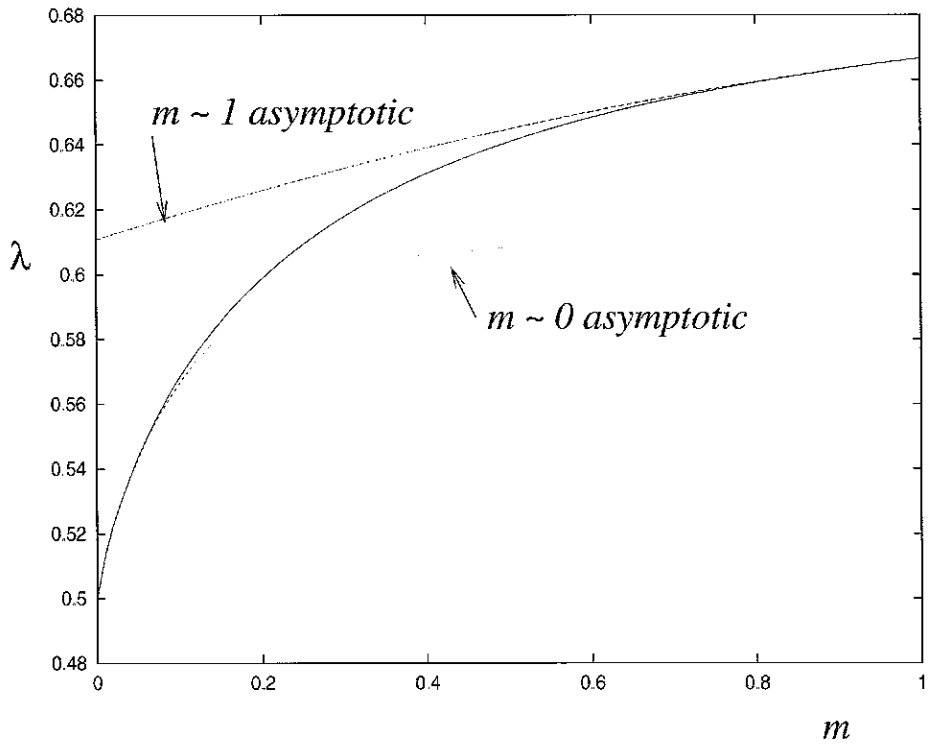


*Figure 3* Dependence of $\lambda$ upon $m$ (solid line) and asymptotic estimates (14) and (15) (broken lines)

where $z_c = \lambda h$ It may easily be confirmed that (13) has a unique solution $1/2 < \lambda \leq 2/3$ for all $m$ with $0 < m \leq 1$, and this solution may easily be located using any standard numerical method for solving a single nonlinear equation. It is also a simple matter to determine the behaviour of $\lambda$ when $m$ is close to 0 or 1 ('asymptotics on the asymptotics'). We find that

$$\lambda = \tfrac{2}{3} + \tfrac{1}{27}(1 - \tfrac{8}{3}\log 2)(1-m) + \\ + \tfrac{1}{81}(1 - 4\log 2 - \tfrac{4}{9}(\log 2)^2)(1-m)^2 + O((1-m)^3) \quad (m \sim 1), \tag{14}$$

$$\lambda = \frac{1}{2} - \frac{m}{4}\log m + \frac{\log 2}{4}m + \frac{3}{8}m^2 \log m + O(m^2) \quad (m \sim 0). \tag{15}$$

The parameter $\lambda$ is shown as a function of $m$ along with the asymptotic estimates (14) and (15) in Figure 3. It may also be confirmed from (8) and (9) that for a given $m$, $u = 0$ at $z = (2\lambda - 1)h$.

Once $\lambda$ is known, $p_x$ is determined for a given $U$ by (12) (and is a constant). We find that

$$p_x = \frac{\mu_0}{h^{1+m}} \left( \frac{(1+2m)U\lambda}{m[\lambda^{\frac{1+2m}{m}} + (1-\lambda)^{\frac{1+2m}{m}}]} \right)^m \tag{16}$$

Having determined $u$, we may now turn to the $y$-momentum equation (5). We must solve

$$p_y = (\mu_0 (u_z^2)^{\frac{m-1}{2}} v_z)_z$$

with $v = 0$ at $z = 0$ and $z = h$, and once again this may be accomplished by simple integration. Again we solve separately for the two regions $0 \leq z \leq z_c$ and $z_c \leq z \leq h$ and use the boundary conditions $v_z = 0$, $v$ continuous at $z = z_c$. This gives

$$v = \begin{cases} \dfrac{mp_y p_x^{\frac{1-m}{m}}[(z_c - z)^{\frac{1}{m}}(-(z-h)(h-z_c)^{\frac{1}{m}} - zz_c^{\frac{1}{m}}) - hz_c^{\frac{1}{m}}(h-z_c)^{\frac{1}{m}}]}{(1+m)\mu_o^{\frac{1}{m}} h^{\frac{1}{m}}[\lambda^{\frac{1}{m}} + (1-\lambda)^{\frac{1}{m}}]} & (z \le z_c) \\ \dfrac{mp_y p_x^{\frac{1-m}{m}}[(z - z_c)^{\frac{1}{m}}((z-h)(h-z_c)^{\frac{1}{m}} + zz_c^{\frac{1}{m}}) - hz_c^{\frac{1}{m}}(h-z_c)^{\frac{1}{m}}]}{(1+m)\mu_o^{\frac{1}{m}} h^{\frac{1}{m}}[\lambda^{\frac{1}{m}} + (1-\lambda)^{\frac{1}{m}}]} & (z \ge z_c) \end{cases}$$

The throughput $\mathcal{T}_1$ (measured in kg m$^{-1}$ s$^{-1}$) may now be found. (Here and henceforth we work, unless otherwise stated, in terms of the throughput due to the portion of the device *between two scrapers*. This value should be multiplied by the number of scrapers and the distance between adjacent scrapers to determine the total device mass flux (kg s$^{-1}$).) We have

$$\mathcal{T}_1 = \rho \int_0^h v \, \mathrm{d}z$$

and, after some calculation, we find that

$$\mathcal{T}_1 = \frac{-\rho p_y h^{2+m} U^{1-m}}{\mu_0} f_1(\lambda, m), \tag{17}$$

where $f_1$ (which depends only on $m$ and $\lambda$) is defined by

$$f_1(\lambda, m) = \frac{m^m \lambda^{1-m}[m^2\Gamma(\lambda^{2+1/m} + (1-\lambda)^{2+1/m}) + (1+2m)\lambda^{1/m}(1-\lambda)^{1/m}]}{(1+2m)^m(1+m)^2\Gamma[\lambda^{2+1/m} + (1-\lambda)^{2+1/m}]^{1-m}}$$

and

$$\Gamma = \lambda^{1/m} + (1-\lambda)^{1/m}.$$

The quantity $\mathcal{T}_1$ depends on the problem parameters in a revealing manner; the dependence on $U$ becomes more greatly pronounced as $m$ decreases (and so the fluid 'shear-thins' by a greater amount) but otherwise $\mathcal{T}_1$ depends linearly on $\rho$ and the pressure gradient.

### 3.1 Newtonian case ($m = 1$)

A partial check of the results derived so far is provided by setting $m = 1$ in the results derived so far to retrieve the Newtonian version of the flow. We find that

$$u = \frac{U(h-3z)(h-z)}{h^2}, \quad v = \frac{p_y z(z-h)}{2\mu_0},$$

$$z_c = \frac{2h}{3}, \quad p_x = \frac{6\mu_0 U}{h^2}, \quad \mathcal{T}_1 = \frac{-p_y \rho h^3}{12\mu_0}$$

Naturally in this limit the throughput is independent of $U$ since now rotating the inner cylinder cannot change the fluid viscosity.

### 3.2. Optimization problem

We may now address (at least, in principle) the optimization problem that was the original focus of this study. We know that

$$\mathcal{T}_1 \propto (-p_y)U^{1-m}$$

and we must choose $U$ and $-p_y = \Delta P$ say to maximize this quantity subject to the total power expenditure being fixed. There are many alternative, but essentially equivalent ways of formulating the optimization problem; we adopt the simplest and assume that the total power expended (measured in W = kg m$^2$ s$^{-3}$) is composed of (a) a component due to the rotation of the inner cylinder and (b) a component due to the maintenance of a pressure gradient via a pump. Using elementary engineering correlations (other more accurate formulae may be found in the literature; see, for example [10]), we now assert that

$P_p$ = pump power = (Volume flow rate)(Pressure difference)

and

$P_r$ = rotation power = (Torque)(Angular velocity).

The total volume flow rate (for a device with three scrapers) is given by $3L\mathcal{T}_1/\rho$, whilst the pressure difference down the device is $D\Delta P$. Thus

$$P_p = \frac{3L(\Delta P)^2 h^{2+m} U^{1-m} D}{\mu_0} f_1(\lambda, m).$$

As far as the torque is concerned, the shear stress $\tau$ may easily be calculated to be given by

$$\tau = \mu_0 (u_z^m)_{z=0} = p_x z_c.$$

With a three-scraper device the force is thus $3Lp_x z_c D$ and the torque is therefore $3Lap_x z_c D$ where $a$ is is the radius of the inner cylinder. The power is thus given by $3LUp_x z_c D$, and using (16) now gives

$$P_r = 3LU^{1+m} D h^{-m} \lambda \mu_0 g(\lambda, m),$$

where

$$g(\lambda, m) = \frac{\lambda^m (1+2m)^m}{m^m [\lambda^{2+1/m} + (1-\lambda)^{2+1/m}]^m}.$$

We now seek to maximise $\Delta P U^{1-m}$ subject to

$$P_r + P_p = P_t, \tag{18}$$

where $P_t$ is the prescribed total available power. Perfect power transmission has been assumed in (18); in reality, for most devices it is reasonable to assume that the ratio of actual power delivered to the power input is a constant, usually known as the efficiency (which may be as low as 0·1 or 0·2; see, for example [11] or [12]). We do not include efficiencies here, but obviously they could easily be incorporated if they were known.

To maximise $\Delta P U^{1-m}$ subject to

$$K_1 U^{1+m} + K_2 (\Delta P)^2 U^{1-m} - P_t = 0,$$

where

$$K_1 = 3LDh^{-m} \mu_o \lambda g(\lambda, m), \quad K_2 = \frac{3Lh^{2+m} D f_1(\lambda, m)}{\mu_0};$$

we introduce a Lagrange multiplier $\phi$ and instead maximize

$$\Delta P U^{1-m} - \phi (K_1 U^{1+m} + K_2 (\Delta P)^2 U^{1-m} - P_t).$$

The three equations to be solved are thus

$$0 = U^{1-m} - 2\phi K_2 \triangle P U^{1-m}, \tag{19}$$

$$0 = (1-m) \triangle P U^{-m} - \phi[(1+m)K_1 U^m + (1-m)K_2(\triangle P)^2 U^{-m}], \tag{20}$$

$$0 = K_1 U^{1+m} + K_2(\triangle P)^2 U^{1-m} - P_t. \tag{21}$$

Solving (19) and (20), we find that

$$\triangle P = \frac{1}{2K_2\phi}, \quad U = \left(\frac{1-m}{4\phi^2(1+m)K_1K_2}\right)^{\frac{1}{2m}}.$$

From (21) we therefore find that $\phi$ satisfies the nonlinear algebraic equation

$$K_1\left(\frac{1-m}{4\phi^2(1+m)K_1K_2}\right)^{\frac{1+m}{2m}} + \frac{1}{4\phi^2K_2}\left(\frac{1-m}{4\phi^2(1+m)K_1K_2}\right)^{\frac{1-m}{2m}} = P_t \tag{22}$$

and the optimization problem is, in principle solved, once (22) is solved.

In a real industrial device the key parameters may take a range of values; here we analyse the predictions of (22) to calculate the optimum values of $U$ and $\triangle P$ for a typical industrial device specification. Assuming that $m = \frac{2}{3}$ (a value typical for margarine, jam and peanut butter) we first solve (13) to give $\lambda \sim 0{\cdot}65250$ whence $f_1(\lambda, m) \sim 0{\cdot}09793$ and $g(\lambda, m) \sim 4{\cdot}37993$. Now we take typical values $\rho = 800\ \mathrm{kg\ m^{-3}}$, $h = 0{\cdot}015$ m, $L = 0{\cdot}15$ m, $D = 2$ m and also assume that $\mu_0 = 10{\cdot}0$ (this value may vary for different food products, but certainly the order of magnitude of this figure is correct). We now have to give a value for the total power $P_t$; we take $P_t = 2{\cdot}5$ kW (a typical value for a medium-sized device that might be used in a factory for food processing). Solving (22), we find that $\phi \sim 31{\cdot}4953$ and the throughput is thus maximised when $U \sim 0{\cdot}9911\ \mathrm{m\ s^{-1}}$ and $\triangle P = 131620{\cdot}4$ Pa, the associated volume flow rate being $3L\mathcal{T}_1/\rho = 0{\cdot}007914\ \mathrm{m^3\ s^{-1}}$. Although detailed information for a range of devices and food products is not available, it may be confirmed that the figures for $U$ and $\triangle P$ are really rather close to the values that have been found by trial and error in factories.

Of course, the real advantage of the current asymptotic formulation is the amount of parameter-dependence information that may be gleaned from (17) and (22). For example, Figure 4 shows the optimal volume flow rate (in $\mathrm{m^3\ s^{-1}}$) as a function of $m$ for the parameters $\rho = 800\ \mathrm{kg\ m^{-3}}$, $P_t = 2{\cdot}5$ kW, $h = 0{\cdot}015$ m, $L = 0{\cdot}15$ m, $D = 2$ m and $\mu_0 = 10{\cdot}0$. As $m$ decreases and the fluid shear-thins to a greater extent, it is clear that the optimum volume flow rate increases dramatically. It may also be confirmed that, as expected, decreasing $m$ also decreases the optimal pressure gradient and increases the value of the optimal rotation speed as it becomes more worthwhile to expend greater amounts of energy in thinning the fluid.

## 4. Analysis for other orders of magnitude of $U$

Though the analysis of the previous section has covered the case that we believe is of most relevance as far as the currently-operated industrial process is concerned, the framework that has been set up to examine the problem allows some other limits to be considered. These are now briefly analyzed for the sake of completeness.

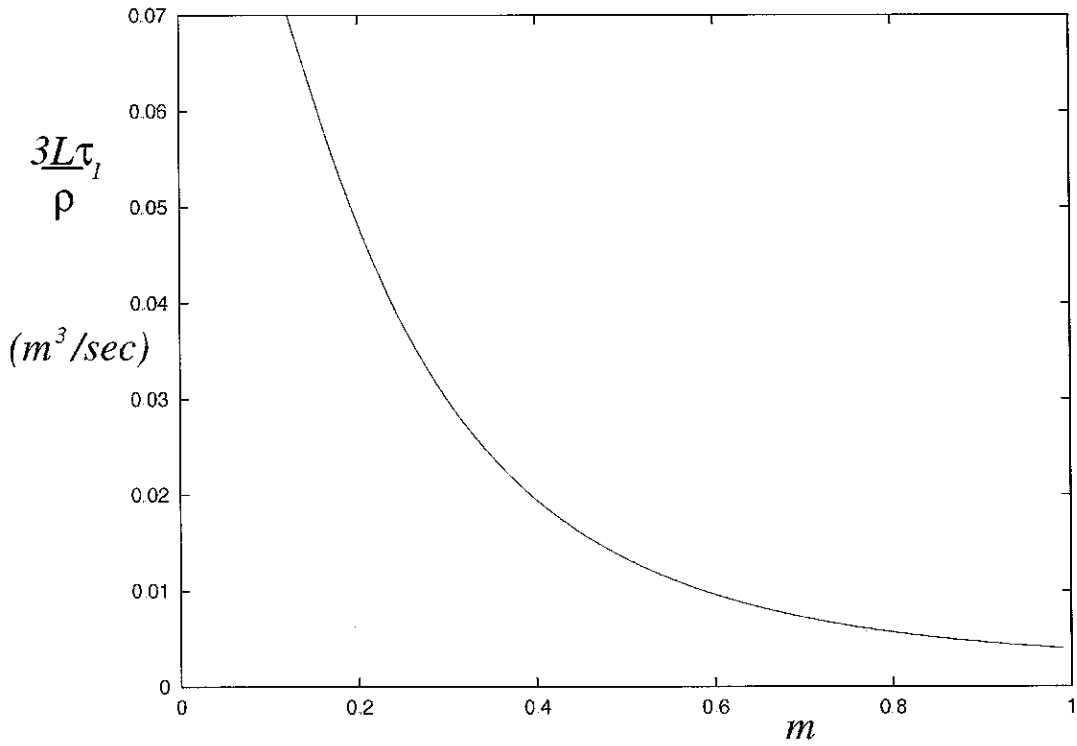


*Figure 4.* Optimum volume flow ($m^3\ s^{-1}$) as a function of shear-thinning exponent $m$

### 4.1 Analysis for small rotation rates

When the rotation rate is very small so that $U$ is not large enough to contribute to the leading order flow, we scale in an identical manner to that discussed at the beginning of Section 3, save for the fact that we set $v = (U/\epsilon)\bar{v}$ and

$$p = \frac{\mu_0 U}{L\epsilon^4}\left(\frac{U}{\epsilon h}\right)^{m-1}\bar{p}.$$

Essentially this scaling may be thought of as one that preserves the previous orders of magnitude of $v$ and $p_y$ for small $U$. The (dimensional) leading-order equations now become

$$0 = -p_x, \quad 0 = -p_y + (\mu_0(v_z^2)^{\frac{m-1}{2}}v_z)_z,$$

$$0 = -p_z, \quad u_x + v_y + w_z = 0$$

and hence the problem reduces to that of determining Poiseuille flow for a shear-thinning fluid. The quantity $p_y$ is therefore a function of $y$ alone (and for the sake of definiteness we will assume here and henceforth that $p_y$ is negative so that flow takes place in a positive direction along the $y$-axis) and we must solve

$$p_y = (\mu_0(v_z^2)^{\frac{m-1}{2}}v_z)_z$$

with $v = 0$ at $z = 0$ and $z = h$. The flow is evidently symmetrical in the regions $0 \le z \le h/2$ and $h/2 \le z \le h$ and may be easily confirmed to be given by

$$v = \begin{cases} \left(\frac{m}{1+m}\right)\left(\frac{-p_y}{\mu_0}\right)^{\frac{1}{m}}\left[\left(\frac{h}{2}\right)^{\frac{1+m}{m}} - \left(\frac{h}{2}-z\right)^{\frac{1+m}{m}}\right] & (0 \le z \le h/2) \\ \left(\frac{m}{1+m}\right)\left(\frac{-p_y}{\mu_0}\right)^{\frac{1}{m}}\left[\left(\frac{h}{2}\right)^{\frac{1+m}{m}} - \left(z-\frac{h}{2}\right)^{\frac{1+m}{m}}\right] & (h/2 \le z \le h) \end{cases}.$$

A 'scraper condition' may be imposed as before to show that the quantity $p_y$ is a constant, however to fully determine $u$ and $w$ it is necessary to consider a higher-order problem. Notwithstanding this, the throughput $\mathcal{T}_2$ may be established; we find by simple integration that

$$\mathcal{T}_2 = \frac{2\rho m(-p_y)^{1/m}h^{2+1/m}}{(1+2m)\mu_0^{1/m}2^{2+1/m}}$$

and we note that, in contrast to the case considered in the previous section, the throughput is now independent of $U$, and depends on the $(1/m)$th power of the quantity $-p_y/\mu_0$.

Finally for this case, we note that setting $m = 1$ to retrieve the Newtonian case once again gives the familiar Poiseuille flow results

$$v = \frac{-p_y}{2\mu_0}z(h-z) \quad (0 \le z \le h),$$

$$\mathcal{T}_2 = \frac{-p_y\rho h^3}{12\mu_0}.$$

### 4.2. Analysis for larger small rotation rates

When $U$ is too small to contribute to the leading-order flow, but large enough to play a role in the shear, an "intermediate case" arises which may be analyzed (and is the distinguished limit containing both of the previous cases). For this case, the relevant scalings are identical to those used at the beginning of Section 3, save for the fact that we set $v = U\bar{v}$ and

$$p = \frac{\mu_0 U}{L\epsilon^3}\left(\frac{U}{h}\right)^{m-1}\bar{p}.$$

As usual, to leading order $p$ cannot depend upon $z$, but in this case we also find that $p$ is independent of $x$. Hence the correct expansion for $p$ is $p = p_0(y) + \epsilon p_1(x, y) + O(\epsilon^2)$. The dimensional pressure gradients in the $x$ and $y$ directions are thus comparable for this intermediate case. If this expansion for the pressure is used the (dimensional) equations governing the leading-order velocities are

$$0 = -p_x + (\mu_0(u_z^2 + v_z^2)^{\frac{m-1}{2}}u_z)_z, \tag{23}$$

$$0 = -p_y + (\mu_0(u_z^2 + v_z^2)^{\frac{m-1}{2}}v_z)_z, \tag{24}$$

$$0 = -p_z, \tag{25}$$

$$0 = u_x + w_z. \tag{26}$$

The major difference between this case and the previous cases that have been discussed is that it is now easy to see that $u_z$ and $v_z$ change sign at distinct positions, which we shall denote by $z = z_c$ and $z = z_b$, respectively. We shall also assume, as usual, that $p_x > 0$ and $p_y < 0$. Integration of (23) and (24) now gives

$$u_z \mu_0 (u_z^2 + v_z^2)^{\frac{m-1}{2}} = (z - z_c) p_x, \tag{27}$$

$$v_z \mu_0 (u_z^2 + v_z^2)^{\frac{m-1}{2}} = (z - z_b) p_y \tag{28}$$

and thus

$$v_z = \frac{u_z}{g}\left(\frac{z - z_b}{z - z_c}\right),$$

where

$$g = \frac{p_x}{p_y} \quad (< 0).$$

This expression for $v_z$ may now be used in (27) to yield an equation for $u_z$. It is simplest to solve this equation separately in the regions $z \geq z_c$ and $z \leq z_c$. We find that

$$u = \begin{cases} \left(\dfrac{p_x}{\mu_0}\right)^{\frac{1}{m}} (-g)^{\frac{m-1}{m}} [f_c(z) - f_c(0)] + U & (z \leq z_c), \\ \left(\dfrac{p_x}{\mu_0}\right)^{\frac{1}{m}} (-g)^{\frac{m-1}{m}} f_c(z) & (z \geq z_c), \end{cases}$$

where

$$f_c(z) = \int_h^z \frac{s - z_c}{[g^2(s - z_c)^2 + (s - z_b)^2]^{\frac{m-1}{2m}}}\, \mathrm{d}s.$$

The condition that $u$ is continuous at $z = z_c$ now yields

$$U = f_c(0)\left(\frac{p_x}{\mu_0}\right)^{\frac{1}{m}} (-g)^{\frac{m-1}{m}},$$

and the mass flow condition

$$\int_0^h u_x \, \mathrm{d}z = 0$$

imposed by the scrapers once again confirms the hypothesis that $p_x$ is constant, and is given by

$$p_x = \frac{\mu_0 (U z_c)^m}{(-g)^{m-1}\left(z_c f_c(0) - \int_0^h f_c(z)\, \mathrm{d}z\right)^m}$$

Now that $u$ has been determined, $v$ may be found in a similar fashion. We find that

$$v = \begin{cases} \left(\dfrac{-p_y}{\mu_0}\right)^{\frac{1}{m}} f_b(z) & (z \leq z_b) \\ \left(\dfrac{-p_y}{\mu_0}\right)^{\frac{1}{m}} [f_b(z) - f_b(h)] & (z \geq z_b) \end{cases},$$

where

$$f_b(z) = \int_0^z \frac{z_b - s}{[g^2(s - z_c)^2 + (s - z_b)^2]^{\frac{m-1}{2m}}}\,\mathrm{d}s$$

and the condition that $v$ is continuous at $z = z_b$ requires that $f_b(h) = 0$. The problem is now, in principle, solved. For a given imposed pressure gradient $p_y$ we must solve

$$U = \left(\int_h^0 \frac{s - z_c}{[g^2(s - z_c)^2 + (s - z_b)^2]^{\frac{m-1}{2m}}}\,\mathrm{d}s\right)\left(\frac{p_x}{\mu_0}\right)^{\frac{1}{m}}\left(\frac{p_x}{-p_y}\right)^{\frac{m-1}{m}}, \tag{29}$$

$$p_x = \frac{\mu_0(Uz_c)^m}{(-g)^{m-1}\left(z_c f_c(0) - \int_0^h f_c(z)\,\mathrm{d}z\right)^m}, \tag{30}$$

$$0 = \int_0^h \frac{z_b - s}{[g^2(s - z_c)^2 + (s - z_b)^2]^{\frac{m-1}{2m}}}\,\mathrm{d}s \tag{31}$$

to determine $p_x$, $z_b$ and $z_c$; the throughput $\mathcal{T}_3$ is then given by

$$\mathcal{T}_3 = \rho\int_0^h v\,\mathrm{d}z = \rho\left(\frac{-p_y}{\mu_0}\right)^{\frac{1}{m}}\left[\int_0^h f_b(z)\,\mathrm{d}z\right]. \tag{32}$$

Each of (29–31) and (32) may be simplified: when we set $z_b = \lambda_b h$ and $z_c = \lambda_c h$, change the order of integration in (30) and (32) and use some elementary properties of the functions $f_b$ and $f_c$, some straightforward algebra reveals that in the most convenient formulation of the problem the throughput $\mathcal{T}_3$ may be expressed as

$$\mathcal{T}_3 = \frac{\rho\lambda_b U h}{(-g)},$$

where $g$, $\lambda_b$ and $\lambda_c$ satisfy the nonlinear equations

$$\int_0^1 \frac{s(s - \lambda_c)}{[g^2(s - \lambda_c)^2 + (s - \lambda_b)^2]^{\frac{m-1}{2m}}}\,\mathrm{d}s = 0, \tag{33}$$

$$\int_0^1 \frac{\lambda_b - s}{[g^2(s - \lambda_c)^2 + (s - \lambda_b)^2]^{\frac{m-1}{2m}}}\,\mathrm{d}s = 0, \tag{34}$$

$$\int_0^1 \frac{\lambda_c - s}{[g^2(s - \lambda_c)^2 + (s - \lambda_b)^2]^{\frac{m-1}{2m}}}\,\mathrm{d}s = \frac{\alpha}{(-g)} \tag{35}$$

and

$$\alpha = \left(\frac{\mu_0}{-p_y}\right)^{\frac{1}{m}}\frac{U}{h^{\frac{1+m}{m}}}. \tag{36}$$

Unlike the previous two cases that were considered, the parameters $\lambda_b$ and $\lambda_c$ are not now determined solely by $m$; the intimate coupling of $u$ and $v$ now means that even for fixed $m$ the flow will be different for each value of $\alpha$.

Equations (33–35) may be presented in various different forms (for example, judicious combination of (34) and (35) allows a transcendental equation for $\lambda_b$, $\lambda_c$ and $g$ to be derived) but in general it is impossible to avoid the need to solve nonlinear equations that involve integrals. This may be accomplished in an efficient manner by using library routines. For the results presented below, the NAG quadrature routine D01AHF (Patterson's method) was used to evaluate the integrals and the nonlinear equation solver C05NBF (which uses the MINPACK routine HYBRD1; for details see [13]) was used to solve the equations. In all cases solutions to (33–35) proved to be quick to determine, though for values of $m$ near to zero a good initial guess (best provided from computed results for nearby small $m$-values) is required.

### 4.3. Unified throughput law

Although the optimization problem that is most relevant to the the real industrial problem has already been solved in Section 3.2, it is of some interest to gather together the throughput laws for each of three asymptotic cases that have been considered. The most informative way to plot throughput against pressure gradient and rotation speed is to plot the normalised throughput $\bar{\mathcal{T}}$, defined by

$$\bar{\mathcal{T}} = \frac{\mathcal{T}(\mu_0)^{\frac{1}{m}}}{\rho(-p_y)^{\frac{1}{m}} h^{\frac{1+2m}{m}}}$$

against $\alpha$ as defined in (36). In Figure 5, the quantities

$$\bar{\mathcal{T}}_1 = f_1(\lambda, m)\alpha^{1-m}, \quad \bar{\mathcal{T}}_2 = \left(\frac{m}{1+2m}\right) 2^{-1-1/m}, \quad \bar{\mathcal{T}}_3 = \frac{\lambda_b \alpha}{(-g)}$$

are plotted against $\alpha$ for $m = 0{\cdot}3$ (broken line) and $m = 0{\cdot}6$ (dot-dashed line). In each case the horizontal line denotes $\mathcal{T}_2$ which is independent of $\alpha$. (The solid line shows the throughput for the Newtonian case for purposes of comparison; of course, when $m = 1$, $\mathcal{T}_1$, $\mathcal{T}_2$ and $\mathcal{T}_3$ are identical.) For both $m = 0{\cdot}3$ and $m = 0{\cdot}6$ the higher of the two non-constant throughput curves corresponds to $\mathcal{T}_3$ and the lower to $\mathcal{T}_1$; when $\alpha \ll 1$ the quantity $\mathcal{T}_1$ tends to zero, rather than the correct value $\mathcal{T}_2$. The asymptotics give us a great deal of information about the throughput of the device; the parametric dependence is rather subtle, and may be too involved to be detected by all but the most careful experimental or numerical studies.

## 5. Enhanced modelling of scrapers

Thus far we have assumed that the scrapers located on the outer cylinder allow no fluid to pass through them. Though it is true that such scrapers really *are* designed to literally scrape the inner cylinder clean of any material (and thus contact with the inner cylinder is constantly maintained), for design reasons it is sometimes necessary to manufacture scrapers that contain holes. If we wished to analyse such a device, the models presented above could easily be modified by altering the scraper condition (10). The simplest way of modelling perforated scrapers would be to use a scraper condition of the form

$$\int_0^h u_x \, \mathrm{d}z = Q,$$

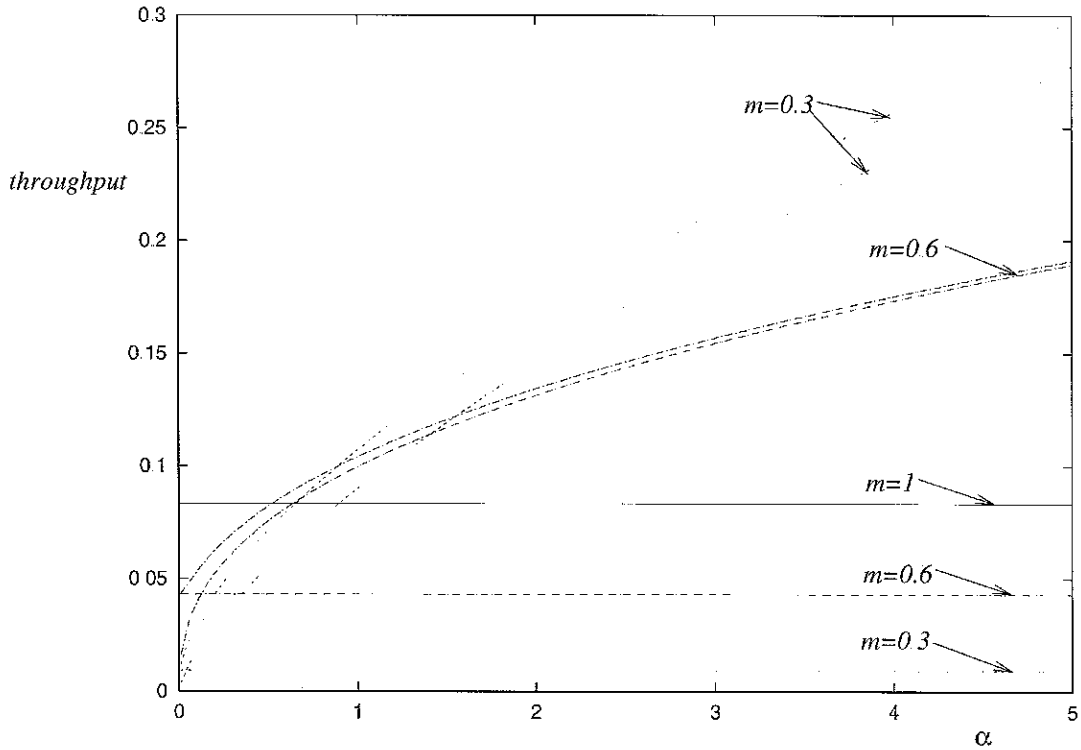


*Figure 5.* Non-dimensional throughputs $\mathcal{T}_1$, $\mathcal{T}_2$ and $\mathcal{T}_3$ for $m = 0{\cdot}3$ (broken line) and $m = 0{\cdot}6$ (dot-dashed line) (see text)

where $Q$ is the mass loss through a scraper, which we assume in known. More elaborate models might also be posed in which $Q$ depended on the pressure drop across a scraper. The main change to the analysis presented above would be that $p_x$ would now no longer be constant; apart from this, however, our previous analysis would carry through in more or less the same form.

As far as asymptotic analysis is concerned, there is also scope for further treatment of the scrapers. Near to a scraper, it is clear that the flow adjacent to the inner cylinder amounts to the classical 'driven flow in a corner' problem where flow is produced by moving a wall parallel to itself. It has long been known that for Newtonian flow ($m = 1$) a simple exact solution is available (see, for example [14]). Recently, it was shown ([15]) that the problem could be solved for a shear-thinning fluid in the limit $m \to 0$. Moreover, the resulting predictions remained remarkably accurate even for values of $m$ quite close to 1. (See also [14].) It could therefore reasonably be observed that asymptotic methods have succeeded for this part of the problem also.

In the region near to a scraper but adjacent to the wall of the outer cylinder, we may expect to observe recirculating eddies. For a Newtonian flow, this problem was solved completely in [16]; at present, however, little progress appears to have been made in solving this problem for shear-thinning flows (though see, for example, [14] and [17]).

## 6. Numerical calculations

We have already seen that some of the details of the parametric dependence of the throughput etc. are rather subtle and involved. Is it therefore possible that the results of all the asymptotic work described above could be predicted solely by a numerical attack on the problem? Let us consider what sort of numerical work could be undertaken. First, we could produce made-to-measure codes to examine various aspects of the problem. This would allow us to carry out careful and accurate numerical calculations to determine the throughput, find what the flow in a cross-section looks like, examine the flow near a scraper, etc. The disadvantage of an investigation of this sort is that many different codes will have to be written, as different numerical schemes may have to be used in different parts of the flow. If the company is question is NASA and the product is the space shuttle, then detailed investigation of this sort may be feasible. For a small industrial concern, however, a second option is more viable: to use a commercial code.

To remain true to the industrial background of this problem, we have therefore used an off-the-shelf package to perform numerical calculations. We chose to use FASTFLO™ (see, for example [18]) because rather than being a 'black box' CFD code it is essentially a finite–element partial differential equation solver. This allows the user to take more control of the calculations by specifying the mesh, method and tolerances that are to be used. It is worth pointing out that although we decided to solve the full problem (*i.e.* with inertia included) some numerical simplifications may result if only the slow flow problem is tackled.

For all the calculations below, an Augmented Lagrangian Method (ALM) was coded into FASTFLO™. The ALM method (for a full explanation see, for example [19] or standard CFD texts) solves the (Newtonian) non-dimensional Navier–Stokes equations

$$\mathrm{Re}(\bar{\boldsymbol{q}}.\bar{\nabla})\bar{\boldsymbol{q}} = -\bar{\nabla}\bar{p} + \bar{\nabla}^2\bar{\boldsymbol{q}}, \quad \bar{\nabla}.\bar{\boldsymbol{q}} = 0$$

by using the iterative procedure

$$-\mathrm{Pen}\bar{\nabla}(\bar{\nabla}\,\bar{\boldsymbol{q}}_n) + \bar{\nabla}\bar{p}_{n-1} - \bar{\nabla}^2\bar{\boldsymbol{q}}_n + \mathrm{Re}\bar{\boldsymbol{q}}_{n-1}.\bar{\nabla}\bar{\boldsymbol{q}}_n = 0, \tag{37}$$

$$\bar{p}_n = \bar{p}_{n-1} - \mathrm{Pen}\bar{\nabla}.\bar{\boldsymbol{q}}_n$$

for $n = 0, 1, \ldots$ where Pen is a 'Penalty parameter' and we denote non-dimensional variables as usual using an overbar. The method is more accurate and reliable than the popular 'penalty' method as there are no restrictions on the size of the penalty parameter. Also, in contrast to the penalty method, the algorithm (if it converges) introduces no further errors into the calculation and provides a solution for the pressure. The alterations that must be made to the algorithm for shear-thinning flow are of a fairly minor nature: in addition to the inclusion of the nonlinear terms in (37) an initial estimate for the viscosity must be provided. All of the calculations detailed below were carried out on a P200 microcomputer running the LINUX version of FASTFLO™.

### 6.1. Cross-sectional flow comparisons

We first used FASTFLO™ to make numerical/asymptotic comparisons for the cross-sectional flow between two scrapers. Computations were performed in a box of aspect ratio 1·10, the bottom wall moving with a speed of 1 parallel to itself. The finite-element mesh was composed of six-noded triangles (quadratic element) and had 500 corner nodes. The penalty parameter

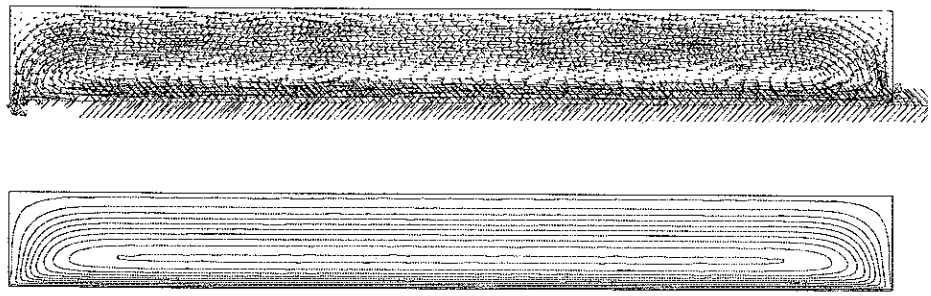

*Figure 6.* Numerical results (arrow plot, streamline plot) for $m = \frac{2}{3}$

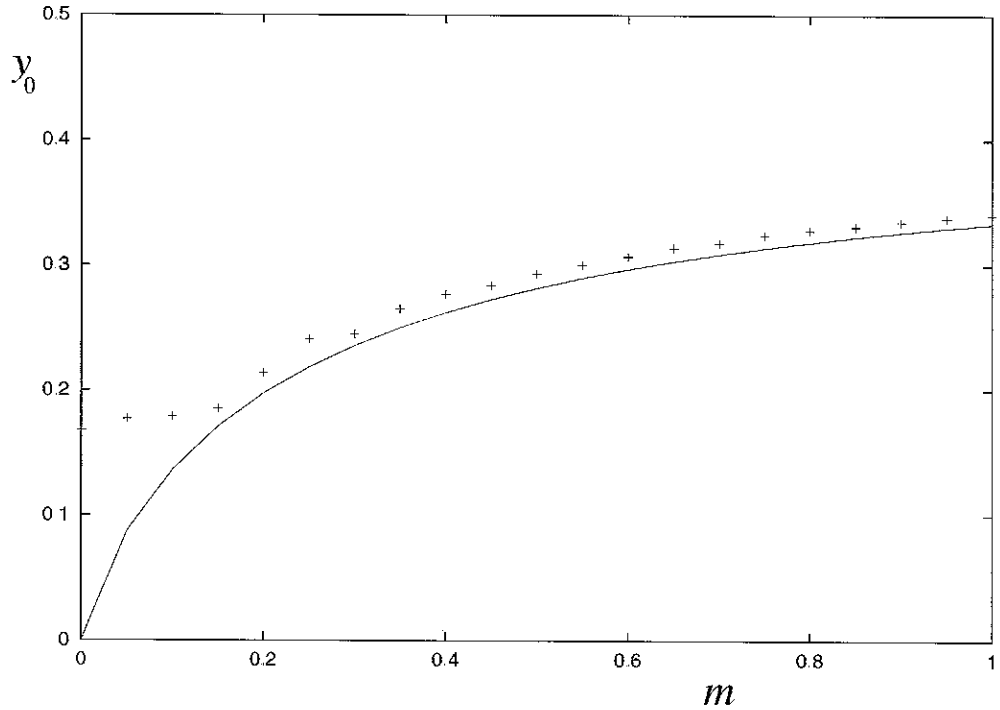


*Figure 7* Ordinate $y_0$ where horizontal velocity $u$ is zero Numerical results (symbols) and asymptotic predictions (solid line) *vs* $m$

was taken to be Pen = 200. Computations typically converged in 10–20 iterations (using about a minute of CPU time) and the usual convergence checks were made by ensuring that as the number of mesh elements increased the converged solutions became indistinguishable.

Figure 6 shows typical numerical results (in the form of a velocity arrow plot and a streamline plot) for $m = \frac{2}{3}$. Although there are some inherent problems in presenting results for a flow region with a 10:1 aspect ratio and individual arrows are hard to distinguish, we note that the flow seems to be independent of $x$ except for regions near to the edges of the box. For the vast majority of the flow, therefore the asymptotic results should be accurate Both of the plots in Figure 6 also clearly indicate the region where the horizontal velocity changes sign. A quantitative comparison between the numerical and asymptotic results may be carried out by comparing the positions $y_0$ where $u = 0$ for different $m$

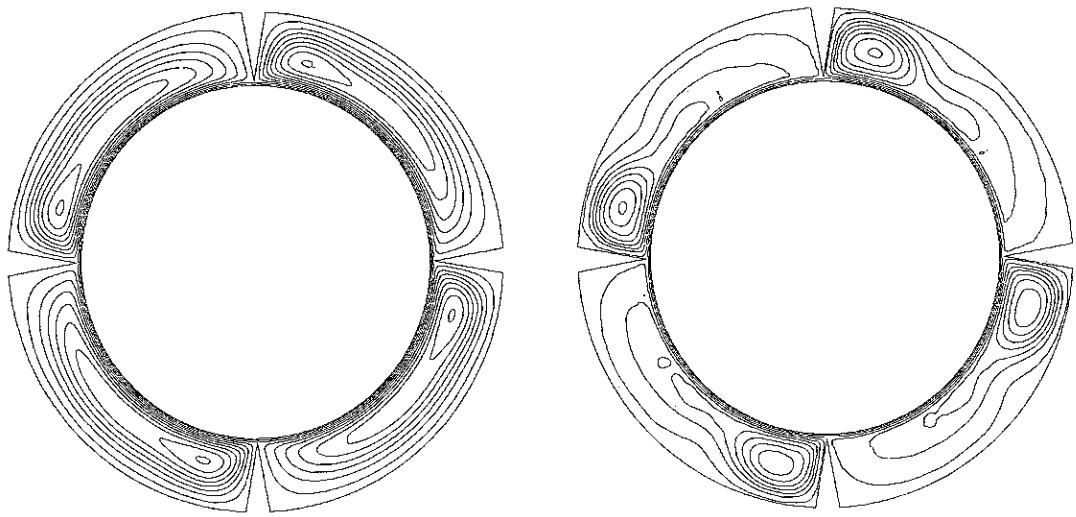

*Figure 8.* Numerical results (streamlines) for four-scraper device with inner cylinder rotating anti-clockwise with non-dimensional speed $\bar{u} = 100$ (Left-hand: Newtonian, right-hand: $m = \frac{2}{3}$)

In Figure 7 $y_0$ is plotted for various $m$ for the same 10:1 aspect ratio box and the same numerical parameters that were used to produce Figure 6. The symbols denote numerically calculated points, and the solid line is the asymptotic theory developed in Section 3. We note that for most values of $m$ the agreement between the symbols and the asymptotic results is excellent. It is no surprise that for small values of $m$, the numerical results seem to be rather unreliable; the computation of shear-thinning flow for small values of the shear-thinning parameter is a notoriously difficult problem. In any case, when $m \ll 1$ there is no guarantee that the asymptotic results are correct anyway, as $m$ is now an additional small parameter in the problem and there are a number of different distinguished limits that may be relevant. Some further numerical experiments (not shown here) are revealing The slightly larger values of $y_0$ that are predicted by the numerical code do not seem to be a result of the discretization, but are rather a consequence of the regions near to the scrapers where the full Navier-Stokes equations apply. Although it is virtually impossible to tell from Figure 6, the effect of these end regions seems to be to slightly increase the value of $y_0$ near to the centre of the flow region, whilst slightly decreasing it closer to the edges of the flow region.

### 6.2 Numerical results for more complicated flow conditions

Although we have tackled many aspects of the problem successfully using asymptotic analysis, there are inevitably some cases where asymptotic analysis does not seem appropriate. As discussed in the introduction, we have to be realistic about what asymptotics can accomplish for us, and there are some device configurations where numerical analysis is our only hope. Figure 8 shows numerical results (streamlines) for a (symmetrical, two-dimensional) four-scraper device where there is a small gap beneath each scraper. The inner cylinder rotates with a non-dimensional speed of 100, so that inertia is no longer negligible. Clearly in this case the shear-thinning nature of the fluid is crucial and changes the flow structure a good deal.

## 7. Conclusions and further work

In this study we have examined only the simplest possible incarnation of the problem of determining the flow of shear-thinning foodstuffs in annular scraped heat exchangers. The geometry of the device clearly allows many simplifications if an asymptotic approach is used, and though the parametric dependence of the throughputs in the three different regimes could no doubt have been determined by more *ad hoc* methods, the detailed description of the flow that an asymptotic approach provides is likely to prove invaluable for further studies

Of course, not all of the asymptotic possibilities of the problem have been exploited. For example, a regular perturbation scheme could easily be employed to consider the case $m = 1 - \epsilon$ ($\epsilon \ll 1$) to determine the details of 'nearly Newtonian' flow. Although from a mathematical point of view this leads only to some very standard analysis, the results would be of practical importance to the device manufacturers as they would allow corrections to be made to flow rate predictions for foodstuffs with $\epsilon \ll 1$. As discussed above, corner solutions could also be examined to determine the local details of the flow near a scraper, and many other asymptotic limits might usefully be pursued.

In particular, we note that, although for the case of the flow of margarine the shear-thinning index is normally greater than 0 5, in previous work we have been interested in the flow of materials where the shear-thinning index tends to zero (see, for example [20] and [15]) The cases studied above could also be looked upon from an $m \to 0$ perspective As usual, we see that in this limit the flow details are very sensitive to the value of $m$; in particular the throughput can change by an order of magnitude when other flow parameters change only by an order one amount. There is clearly scope for further work here.

The main simplifying assumption in the work presented above, namely isothermality, constitutes a serious shortcoming and needs to be remedied when further work is carried out. A local analysis will be required, and this will eventually have to be coupled in to the full model. It should be noted, however, that a 'rough and ready' approximation to the case where temperature dependence is included may be obtained by allowing $\mu_0$ to be a given function of $y$, thereby assuming that the temperature in the heat exchanger is known and depends only only the distance down the apparatus

## Acknowledgements

The authors are grateful to Nick Hall-Taylor of Crown Chemtech Ltd. for bringing the problem to their attention and to Mike Baines and Leo Pyle of Reading University and Jon Chapman of Oxford University for helpful discussions.

## References

1 N. Hall-Taylor, A model for the behaviour of scraped surface heat exchangers Internal Report, Crown Chemtech Ltd , July (1995)

2. N Hall-Taylor, Experimental results for the rheology pastes and spreads Internal Report, Crown Chemtech Ltd., January (1998).

3 G. Astarita and G Marrucci, *Principles of Non-Newtonian Fluid Mechanics* London· McGraw-Hill (1974) 289pp.

4 M.W Johnson and S. Mangkoesoebroto, Analysis of lubrication theory for the power law fluid *J Tribology, Trans. ASME* 115 (1993) 71–77

5 T.R. Lin, Thermal elastohydrodynamic lubrication of rolling and sliding contacts with a power law fluid. *Wear* 154 (1992) 77–93

6. D Prasad and R.P. Chhabra, Thermal and normal squeezing effects in lubrication of rollers by a power-law fluid. *Wear* 145 (1991) 61–76

7. J.M. Wang and G.B. Jin, The optimum design of the Rayleigh slider bearing with a power law fluid. *Wear* 129 (1989) 1–11

8. P. Szabo and O. Hassager, Flow of viscoplastic fluids in eccentric annular geometries. *J Non-Newtonian Fluid Mech.* 45 (1992) 149–169

9 S.H. Bittleston and O. Hassager, Flow of viscoplastic fluids in a rotating concentric annulus. *J Non-Newtonian Fluid Mech.* 42 (1992) 19–36.

10 R.H. Warring, *Pumps: Selection, Systems and Applications, 2nd Ed.* Morden, Surrey: Trade & Technical Press Ltd. (1984) 271pp

11 V.S. Lobanoff and R.R. Ross, *Centrifugal Pumps, Design and Application.* Houston, Texas: Gulf Publications (1985) 374pp.

12 J. Davidson and O. von Bertele, *Process Pump Selection.* UK: Professional Engineering Publishing (2000) 202pp

13 M.J.D. Powell, A hybrid method for nonlinear algebraic equations, In: P. Rabinowitz, (ed.) *Numerical Methods for Nonlinear Algebraic Equations*, Gordon & Breach (1970) pp. 45–48

14. R.T. Fenner, On local solutions to non-Newtonian viscous flows. *Int. J. Non-Linear Mechanics* 10 (1975) 207–214.

15 S.J. Chapman, A.D. Fitt and C.P. Please, Extrusion of power-law shear-thinning fluids with small exponent. *Int. J. Non-Linear Mechanics* 32 (1997) 187–199

16. H.K. Moffatt, Viscous and resistive eddies near a sharp corner. *J. Fluid Mech.* 18 (1964) 1–18.

17 P. Henriksen and O. Hassager, Corner flow of power law fluids. *J. Rheology* 33 (1989) 865–879

18. NAG Ltd., *FASTFLO User Manual.* Oxford, England: Numerical Algorithms Group (1999).

19 X. Nicolas, P. Traore, A. Mojtabi and J.P. Caltagirone, Augmented Lagrangian method and open boundary conditions in 2D simulation of Poiseuille–Bernard channel flow. *Int. J. Num. Meth. Fluid Mech.* 25 (1997) 265–283

20. M.E. Brewster, S.J. Chapman, A.D. Fitt and C.P. Please, Asymptotics of very small exponent power-law shear-thinning fluids in a wedge. *Euro. J. Appl. Math.* 6 (1995) 559–571